Sensitivity Analysis of Half-Bead and Alternative GTAW Techniques

The alternative six-layer technique displays a tolerance to the variables of welding

BY P. J. ALBERRY

ABSTRACT. The ASME XI shielded metal arc half-bead technique and an alternative, mechanized, six-layer gas tungsten arc technique have been assessed using a computer model sensitivity analysis. These techniques have been developed for repair welding of heavy-section steel components in light water reactors without postweld heat treatment. The as-welded heat-affected zones are compared in terms of structure, grain size and hardness. The likely sensitivity of each technique to systematic and random variations in welding parameters is assessed.

Introduction

In 1979, EPRI initiated a research contract EPRI-RP 1236 entitled "Repair Welding of Heavy Section Steel Nozzles" for Babcock and Wilcox, Alliance, Ohio. This project was designed to define and validate an alternative to the ASME XI half-bead repair procedure for light water reactor nozzles. Both repair procedures are intended for use without postweld heat treatment. The half-bead procedure uses a layer-by-layer refinement and tempering technique and is carried out manually. Half of the first layer of weld metal is ground off manually to facilitate the refinement and tempering action of subsequent layers. The heavy dependence on time-consuming manual activities was considered to be a serious practical limitation in reactor environment due to the prolonged exposure to radioactivity. Consequently, with the use of a computer model, an alternative GTAW technique capable of mechanization was designed. The computer model work was carried out in three phases. The first phase was to establish the basic welding metallurgy for SA508 Class 2 heat-affected zones (Ref. 1). The second phase was to use the computer model to develop a viable gas tungsten arc welding (GTAW) procedure (Ref. 2). The third phase, a computer model sensitivity analysis of the likely variability of the ASME XI half-bead technique and the alternative GTAW technique, is reported here.

P. J. ALBERRY is with Marchwood Engineering Laboratories, Central Electricity Generating Board, Marchwood, Southhampton, England.

Computer Model

General Description

Details of the computer model for the prediction of weld heat-affected zone (HAZ) structures and hardnesses produced by the SMA and GTAW processes have been given previously (Refs. 2–4).

Weld HAZ's in a given material consist of a range of structures that reflect the range of thermal cycles experienced. Thermal cycles with peak temperatures close to the melting point are experienced near the weld metal fusion boundary and usually result in the formation of coarse-grained structures. At greater distances from the fusion boundary, the thermal cycle peak temperatures decrease progressively and more fine-grained structures are formed. Eventually, the thermal cycle peak temperature decreases below the Ac_1 and the base material structure is only tempered. This basic unit for a single weld bead is shown in Fig. 1.

In multipass welds, the HAZ formed by the deposition of a single weld bead is modified by the superposition of successive adjacent weld bead deposits. The second thermal cycle modifies the structure of the primary HAZ. Subsequently, thermal cycles may cause further changes, which can involve transformation and tempering, depending on the peak temperatures experienced.

KEY WORDS

Sensitivity Analysis
Half-Bead GTAW
Alternative GTAW
Six-Layer GTA Weld
Computer Model
Repair Welding
Heavy Section Steel
Light Water Reactor
GTAW Sensitivity
Weld HAZ Comparisons

The precise microstructure and hardness at any given point in the HAZ will be determined by its thermal history, grain growth kinetics, phase transformation and tempering behavior. The thermal history will depend upon the welding conditions, joint geometry, spatial positioning of the weld beads, the weld bead shape and the resultant overlap of their HAZ's. Grain growth kinetics are a function of the original structure and time at temperature. The phase transformation and tempering behavior are determined by chemical composition, the prior structure, the austenite grain growth kinetics, the peak austenitizing temperature and the heating and cooling rates during the thermal cycle(s).

Thus, to define the structure and, hence, properties obtained in the HAZ of a given material composition, it is necessary to describe: 1) weld bead shape, 2) the thermal cycle as a function of welding procedure in all regions of the HAZ, 3) prior austenite grain growth as a function of prior structure and weld thermal cycle, 4) variations in transformation behavior as a function of thermal cycle and prior austenite grain size, and 5) tempering effects as a function of thermal cycle experienced for a given transformation product.

Elements 3–5 for SA508 Class 2 (Table 1) were characterized (Ref. 1) in detail in Phase 1.

The thermal history can be calculated from standard heat flow equations, but the position of the fusion boundary cannot be calculated accurately. To overcome this, the weld bead dimensions are established for a given range of welding conditions, and the measured position of the fusion boundary is used as a reference point for the heat flow calculations. The HAZ isotherms are thus calculated relative to the known position of the fusion boundary. This ensures that the heat flow calcu-

Table 1—SA508 Class 2 Material Compositions (wt-%)

Element	Half-Bead Repair and Alternative Six-Layer GTAW Repair (Refs. 1, 5) Base Plate	Half-Bead Repair (Ref. 8)	Half-Bead Repair (Ref. 9)
C	0.23	0.24	0.22
Mn	0.62	0.78	0.80
P	0.010	0.004	0.008
S	0.018	0.011	0.006
Si	0.17 (0.31)[a]	–	0.27
Ni	0.95 (0.39)[a]	0.87	0.85
Cr	0.28	0.45	0.36
Mo	0.70	0.63	0.59
V	0.01	–	<0.01
Nb	0.01	–	–
Al	0.017	–	–
Ti	0.01	–	–
B	0.001	–	–
Cu	0.062	–	–
Sn	0.015	–	–
As	0.020	–	–
Sb	–	–	–

(a) Main segregated elements.

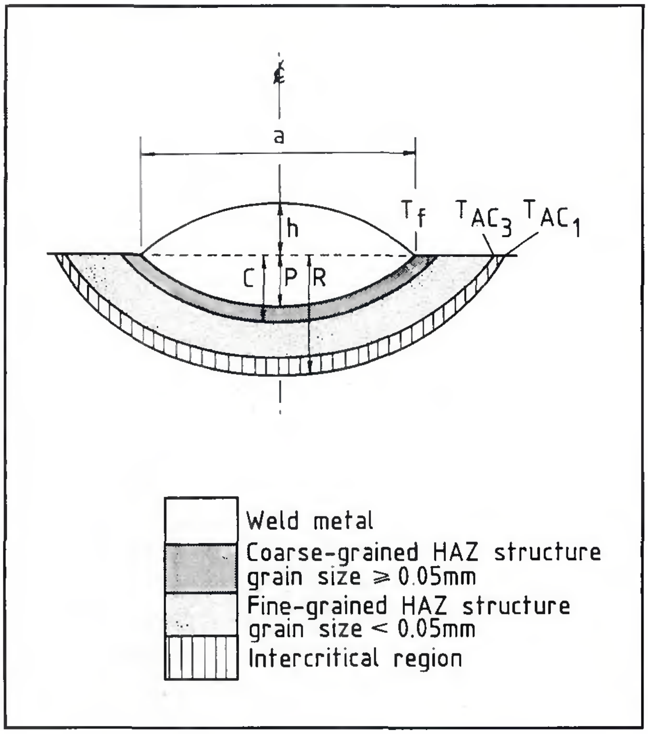

Fig. 1 — Schematic single weld bead and HAZ structure

lations are carried out in that region of the HAZ where conduction heat transfer dominates. This provides a better estimate of the spatial position of the fusion boundary and associated HAZ relative to the plate surface than would be achieved using heat flow calculations alone.

The detailed methodology and algorithms (Ref. 2) used in the model have been validated against a number of shielded metal arc (SMA) and gas tungsten arc (GTAW) procedures (Ref. 5). However, the more important features relevant to the sensitivity analysis are summarized below.

Mean Weld Bead Dimensions and Weld Bead Dimension Variability

The computer model used requires algorithms for the description of weld bead shape, which has an idealized geometry as shown in Fig. 1. This has the disadvantage that the model is not generally applicable but is only valid over the range of conditions used to obtain the weld bead dimension data.

The computer model algorithms for the mean weld bead dimensions are expressed as a function of gross heat input, which is defined as:

$$\text{Gross Heat Input (GHI)} = \text{VIv}^{-1} \quad (1)$$

where V is welding voltage, I is the welding current, and v is the travel speed, $\text{mm}\cdot\text{s}^{-1}$ (2.36 in./min).

Empirical straight-line relationships valid over the range of existing data (Refs. 2, 5) obtained from the measured weld bead dimensions using a least-squares regression analysis are:

$$\text{SMA Mean Bead Width} = 0.00640\,(\text{GHI}) + 3.72;\ r = 0.90 \quad (2)$$

$$\text{Mean Bead Height} = 0.00058\,(\text{GHI}) + 1.41;\ r = 0.54 \quad (3)$$

$$\text{Mean Penetration} = 0.00134\,(\text{GHI}) + 0.44;\ r = 0.82 \quad (4)$$

$$\text{GTA Mean Bead Width} = 0.00770\,(\text{GHI}) + 3.54;\ r = 0.95 \quad (5)$$

$$\text{Mean Penetration} = -0.00020\,(\text{GHI}) + 1.48;\ r = 0.13 \quad (6)$$

where bead dimensions are in mm and r is the correlation coefficient.

Since the GTAW process has a continuous wire feed during welding, it is assumed that all the wire is melted and deposited on the plate surface with little spatter and that the top surface of the weld bead can be represented by the arc of a circle. Hence, it can be shown that the weld bead height can be obtained numerically from:

$$\frac{\pi(\text{WD})^2\text{WFS}}{4\text{v}} = 2\left[\left(\frac{\pi}{360}\left(\frac{h}{2}+\frac{a^2}{8h}\right)^2 \sin^{-1}\left(\frac{4ha}{4h^2+a^2}\right)\right) - \left(\frac{a^3}{32h}-\frac{ha}{8}\right)\right] \quad (7)$$

where WD is the wire diameter (mm), WFS is the wire feed speed ($\text{mm}\cdot\text{s}^{-1}$), a is the weld bead width (mm) (Fig. 1), and h is the weld bead height (mm)—Fig. 1.

Equations 2–6 are empirical and have no known physical basis. The low correlation coefficient for Equation 6 reflects the fact that the measured values of penetration are largely independent of gross heat input over the range of welding conditions used. This is not likely to be generally true. However, the model does not require highly accurate deterministic algorithms. The calculated average values of the mean bead dimensions (MBD) have variability, added by a randomizing process by the model to produce the measured scatter in the empirical database. Hence, the randomized values for bead dimensions (RBD) are obtained from an equation of the type

$$\text{RBD} = \text{MBD} + \left(\sqrt{60}\,\left(\Sigma_i^5 r_i/5\right) - 0.5\right)\sigma_{MBD} \quad (8)$$

where r_i is a random number generated in the range 0 to 1, and σ_{MBD} is the measured standard deviation of the mean bead dimension. The randomizing term $\sqrt{60}\,(\Sigma_i^5 r_i/5) - 0.5$ produces random variate values with a mean value of zero and a standard deviation of 1, which have an approximately Gaussian form (Refs. 6, 7).

The values of weld bead dimension variability for the SMAW and GTAW processes used in the investigation are given in Table 2. Since the bead width and bead

Table 2—Weld Bead Dimension Variabilities for the SMAW and GTAW Processes Used in the Sensitivity Analysis

Weld Bead Dimension	SMAW Standard Deviation (mm)	GTAW Standard Deviation (mm)
Bead width	1.1	0.63
Bead height	0.33	0.11[a]
Penetration	0.33	0.37

(a) Typical value.

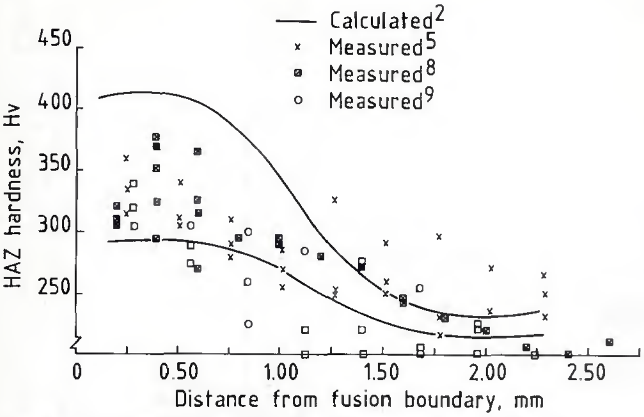

Fig. 2—Measured and calculated HAZ hardness values for the ASME XI half-bead technique

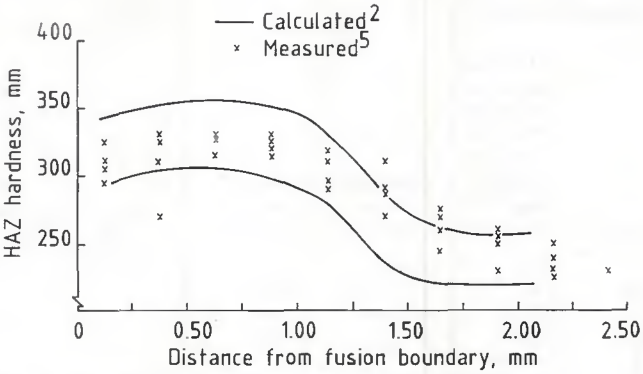

Fig. 3—Measured and calculated hardness values for the alternative six-layer GTAW technique

height are inversely correlated, a randomized value of bead height is obtained from a numerical solution of Equation 7 using the appropriate randomized value of weld bead width together with the appropriate welding conditions.

The computer model now has the capability to examine the effects of weld bead variability on a given weld. Since weld bead variability is the inherent source of weld variability, it allows for the examination of possible weld-to-weld variations, which could be important in some nuclear repair applications. This may help to define the level of experimental validation required to establish a given level of confidence that any given weld is adequately represented by a given set of test samples whose properties are well established.

Table 3—ASME XI Half-Bead Technique Welding Procedure (Ref. 5)

Welding Variables	Welding Conditions[(a)] Layer 1	Layers 2 Onward
Electrode type	E8015-C3	E8015-C3
Current, A	95	140
Voltage, V	25	25
Travel speed, $mm \cdot s^{-1}$	3.39	3.60
Electrode diameter, mm	2.4	3.2
Weld bead overlap, %	50	50
Preheat, °C	177	177
Gross heat input, $J \cdot mm^{-1}$	701	972

(a) Half of the first layer of weld metal is manually ground off before the deposition of Layers 2 onward.

Table 4—Welding Conditions for Six-Layer Alternative GTAW Procedure (Ref. 5)

Welding Parameters	Layer Number 1	2	3–6
Current, A	180	200	220
Voltage, V	11	11	11
Travel Speed, $mm\ s^{-1}$	3.60	2.96	2.54
Wire Feed Speed, $mm\ s^{-1}$	16.5	25.0	27.5
Wire Diameter, mm	0.89	0.89	0.89
Preheat, °C	150	150	150

Model Validation

The computer model described above has the capability to provide detailed hardness distributions across SA508 Class 2 HAZ's for the SMAW and mechanized GTAW processes from a knowledge of the appropriate weld bead dimensions, welding process variables and the basic HAZ metallurgy. The comparison of actual hardness measurements across the HAZ for the SMA half-bead and six-layer mechanized GTA welds (Ref. 5) and the corresponding computer model predictions is now summarized. The full details of the calculations have been described previously (Ref. 2), but sufficient information is given here to provide the basis for the following sensitivity analysis. Note that calculated values of hardness are obtained from computer model calculations based on algorithms that relate to Vickers diamond pyramid hardness (Hv). Hardness measurements (Ref. 5) are Knoop diamond hardness, which are equivalent to Vickers diamond pyramid hardness. An approximate conversion to the Rockwell C scale can be obtained by dividing the Knoop diamond hardness by a factor of 10.

In the ASME XI half-bead technique, the bulk of the refining action is carried out by the second layer, and the bulk of the tempering is carried out by further layers. Details of the ASME XI half-bead weld procedure (Ref. 5) are given in Table 3. A detailed comparison of calculated and measured (Refs. 5, 8, 9) hardness values for the HAZ's corresponding to the base plate compositions given in Table 1 is given in Fig. 2 and shows reasonable agreement. However, the base plate measured hardness values show a wider scatter than predicted. This is not surprising since a significant amount of base plate segregation was reported (Ref. 5), as shown in Table 1.

The alternative six-layer GTAW procedure (Ref. 5) (Table 4) uses the first three added layers to produce refinement and the last three layers to carry out the bulk of the tempering. Computer model hardness predictions across the HAZ are compared with corresponding measurements in Fig. 3. Generally, there is reasonable agreement between the measured and calculated hardness values, and the predicted shape of the hardness traverse band fits the measured data points for maximum HAZ hardnesses to within 10%.

The following sections describe the use of the computer model to provide a sensitivity analysis of the variation in HAZ refinement and peak HAZ hardness with weld parameters.

Sensitivity Analysis

ASME XI Half-Bead Technique HAZ Structure

The continuous cooling transformation data for SA 508 Class 2 HAZ's are available (Ref. 1) for a full range of possible HAZ grain sizes. The bulk of the HAZ produced by the ASME XI half-bead technique is refined with an HAZ grain size of about 0.015 mm and any unrefined areas will have an HAZ grain size of about 0.1 mm. The HAZ structures are predominantly martensite together with a small amount of lower bainite, as shown in Fig. 4. The probability of local unrefined areas can be estimated using the computer model.

HAZ Refinement

The refining action produced by layer-by-layer deposition is illustrated in Fig. 5 where it can be seen that the refining zone of the second layer HAZ continuously penetrates through to the HAZ produced by the first layer. The important refinement parameters are the first layer's average height, the depth of the coarse-grained layer below the original surface, and the penetration of the second layer refining zone. The coarse-grained HAZ extends a few hundred microns only from the fusion boundary; the exact distance depends on the heat input (Ref. 1). Hence, the fusion boundary depth is a convenient first order approximation to the position of the coarse-grained HAZ.

Full refinement of the underlying coarse-grained HAZ will be achieved if

$$P_2 < (GLH_1 + P_1) < R_2$$

where P_1, P_2 are the weld bead penetrations from Layers 1 and 2 respectively.

GLH_1 is the ground layer height of Layer 1, and R_2 is the depth of the refining isotherms from Layer 2.

If $P_2 > (GLH_1 + P_1)$, then the second layer fusion boundary will penetrate past the first layer fusion boundary, producing a second unrefined HAZ appropriate to the welding conditions used to deposit the second layer. This condition is termed overpenetration, which occurs when

$$P_2 - (GLH_1 + P_1) > 0$$

Similarly, if $R_2 < (GLH_1 + P_1)$, then the second layer refining isotherms are located on the weld metal and the first layer coarse-grained HAZ is not refined. This condition is termed underpenetration, which occurs when

$$R_2 - (GLH_1 + P_1) < 0$$

However, the HAZ isotherms are curved, as shown in Fig. 5. This means that there is a maximum and a minimum first layer coarse-grained HAZ depth, a second layer coarse-grained HAZ depth and a refining isotherm depth. Since the bead sizes of the two layers are different, it is not possible to exactly superimpose every second layer weld bead onto every first layer weld bead in the same way. The relative bead positions in the two layers will change progressively. Consequently, when the second layer coarse-grained HAZ falls just short of the maximum coarse-grained HAZ depth of the first layer, then refinement will occur. However, at some other position, the second layer coarse-grained HAZ depth might be sufficient to superimpose itself on the minimum coarse-grained HAZ depth, causing overpenetration. These conditions are defined by different combinations of maxima and minima, as follows:

1) If the maximum coarse-grained HAZ depth is P_1^{max}, then for

overpenetration: $P_2^{max} - (GLH_1 + P_1^{max}) > 0$

underpenetration: $R_2^{min} - (GLH_1 + P_1^{max}) < 0$

2) If the minimum coarse-grained HAZ depth is P_1^{min}, then for

overpenetration: $P_2^{max} - (GLH_1 + P_1^{min}) > 0$

underpenetration: $R_2^{min} - (GLH_1 + P_1^{min}) < 0$

Consequently, the maximum and minimum coarse-grained HAZ depths have different probabilities of being fully refined, *i.e.*, neither overpenetrated nor underpenetrated. However, the probabilities of refinement for the maximum and minimum coarse-grained HAZ depths provide upper and lower bounds for the HAZ as a whole.

The problem is to estimate the probability of overpenetration and underpenetration for the maximum and minimum coarse-grained HAZ depths, given that the weld bead penetrations and isotherm depths are variable. The maximum coarse-grained HAZ depth of Layers 1 and 2 will be taken as equal to their penetration depths. The measured standard deviation of the mean penetration depth is given in Table 2. At a given layer height, assuming perfect grinding, the probability of overpenetration can be calculated by computing the test statistic, x/σ, where x is the overpenetration condition expressed as $0 - (P_2^{max} - (GLH_1 + P_1^{max}))$ and σ is its standard deviation. The overpenetration condition standard deviation is calculated from the individual standard deviations of P_2^{max}, GLH_1 and P_1^{max}, and is given in Table 5. The probability of the test statistic x/σ reaching the critical overpenetration value by chance is obtained from standard tables of the cumulative normal distribution. In this case, this represents the probability that the maximum coarse-grained HAZ depth will be overpenetrated. The probability of underpenetration for the minimum coarse-grained HAZ depth is obtained in the same way. It is clear that the maximum coarse-grained HAZ depth must be either overpenetrated or underpenetrated or fully refined, *i.e.*, Pr (overpenetration) + Pr(underpenetration) + Pr(full refinement) = 1.

Hence, the probability of full refinement being achieved for the maximum coarse-grained HAZ depth is given by 1 - penetration).

The probability of full refinement being achieved for the minimum coarse-grained HAZ depth is obtained in the same way. For the welding conditions given in Table 2, assuming a perfect application of the half-bead technique, the probabilities for full refinement of the maximum and minimum coarse-grained HAZ depths are 0.97 and 0.92, respectively. These probabilities rely on the assumption that half the height of the first layer is ground off with perfect precision. Clearly, this is unlikely to be the case in practice for a weld cavity of variable geometry, in difficult access conditions, in a radioactive environment, at the

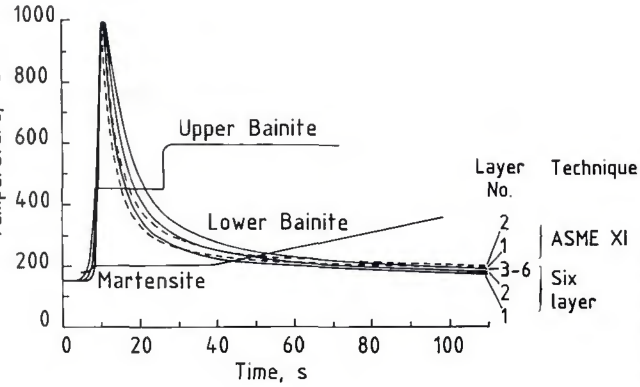

Fig. 4 — Continuous cooling transformation diagram for SA508 Class 2 and superimposed weld

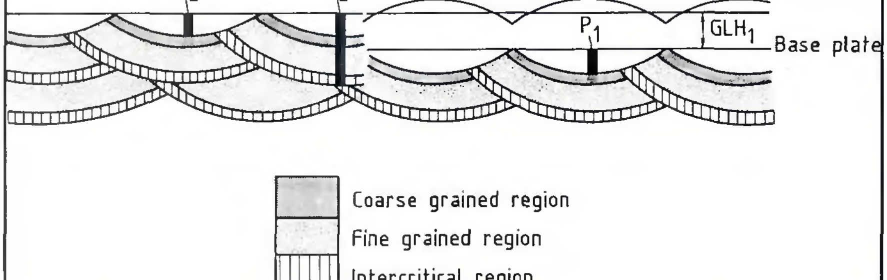

Fig. 5 — Schematic illustration of a two-layer weld showing the superposition of the respective HAZ isotherms

Table 5—Probability of Complete Refinement for the ASME XI Half-Bead Technique

	Maximum	Minimum
First layer penetration P_1, mm	1.38	1.1
Second layer penetration P_2, mm	1.74	–
Second layer refining isotherm depth, R_2, mm	3.86	3.72
Ground layer height GLH_1, mm	1.26	1.26
Overpenetration condition	$P_2^{max} - (GLH_1 + P_1^{max}) > 0$	$P_2^{max} - (GLH_1 + P_1^{min}) > 0$
Standard deviation (σ)	0.45	0.45
Test statistic for overpenetration	2.00	1.38
Probability of overpenetration	0.023	0.084
Underpenetration condition	$R_2^{max} - (GLH_1 + P_1^{max}) < 0$	$R_2^{min} - (GLH_1 + P_1^{min}) < 0$
Standard deviation (σ)	0.45	0.45
Test statistic for underpenetration	2.71	3.02
Probability of underpenetration	0.004	0.001
Probability of full refinement (1-Pr(overpen)-Pr(underpen))	0.97	0.92

weld preheat temperature. The grinding tolerance can be estimated by calculating the probability of full refinement as a function of ground layer height between the extremes where all the first layer weld metal is ground off and where none of the first layer weld metal is ground off. This is shown in Fig. 6. Note that from Fig. 6, the predicted optimum half-bead technique would be a 0.6 bead technique, which would require less grinding for full HAZ refinement.

The effects of systematic variation in welding conditions can also be established in this way. Figure 7 shows the probability of full refinement for systematic errors in welding current, welding voltage and welding travel speed. It is assumed that the same systematic error is present in all layers. Figure 8 shows the probability of full refinement for systematic errors in weld bead overlap, again assuming the same systematic error for both layers. This is reasonable, providing the same welder and welding equipment are used for both layers.

HAZ Hardness

The purpose of the ASME XI half-bead technique is to produce a refined, tempered HAZ. Typical hardness traverses across the HAZ are shown in Fig. 2, which shows scatter typical of multipass welds. The predicted scatter is in reasonable agreement with the results obtained from the computer model. The sensitivity of the peak HAZ hardness produced by given variations in the welding conditions can also be evaluated. In this analysis, it was assumed that the main sources of variation arose from the welder and the grinder. This means that the effects of current and voltage could be neglected, while welding travel speed, weld bead overlap and grinding error were assessed. Furthermore, the welding travel speed and weld bead overlap for Layers 1 and 2 were allowed to vary independently. A series of hypothetical welds were examined using the computer model to evaluate the maximum HAZ hardness produced for a range of welding conditions. A factorial experimental design (Ref. 9) was chosen for this purpose and the actual welding conditions used are given in Table 6, together with the maximum calculated HAZ hardness. Since the main issue was to examine the sensitivity to the effects of the welding parameters, the weld bead variabilities were reduced to zero. This effectively reduced the noise in the computer model system and allowed the effects of each variable to show more clearly, thereby minimizing the computing time. The results were analyzed using a standard factorial analysis, and the effects of each variable were tested for significance at the 95% confidence level. The variance of a single hardness value, V_o, used in the significance test was estimated from the standard deviation of the hardness measurements used to derive the tempering algorithms. The measured standard deviation was 10 Hv 30 kg, which resulted in a variance estimate, V_o, of 100.

The results of the factorial analysis are

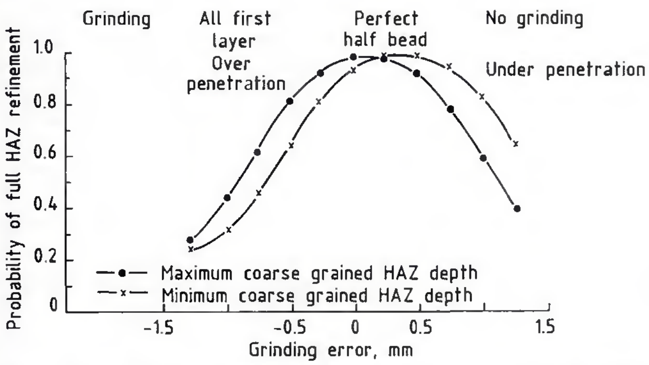

Fig. 6 — Effect of grinding error on the probability of obtaining full HAZ refinement using the ASME XI half-bead technique

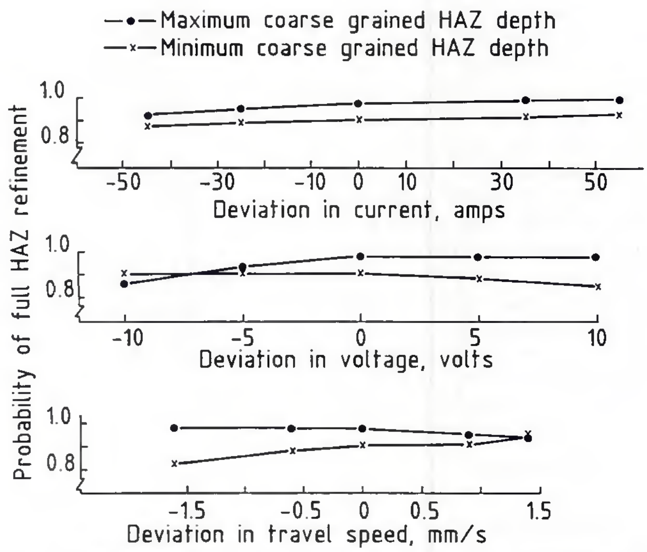

Fig. 7 — Effect of current, voltage and travel speed on the probability of obtaining full HAZ refinement using ASME XI half-bead technique

given in Table 6. The size of each effect given determines its significance, and the sign of each effect determines whether a given input variable combination has a positive or negative effect on the measured response, which in this case is the maximum hardness value for a given traverse across the HAZ. Six input variable combinations have effects that are significant at the 95% confidence level. These are grinding error (− 8.5), second layer travel speed (− 8.6), second layer weld bead overlap (21.5), grinding error and first layer travel speed (11.8), grinding error and first layer weld bead overlap (− 8.5), and second layer travel speed and weld bead overlap (8.5). These effects are complex but a simple interpretation can be obtained in terms of the effect of each parameter on the layer height and the subsequent effect of the change in layer height on the superposition of the HAZ isotherms. For example, increased grinding will reduce the thickness of the first layer. This will cause the isotherms from all subsequent layers to overpenetrate, thereby disturbing the balance of refinement and tempering and resulting in an increase in the maximum hardness.

Decreased grinding will increase the thickness of the first layer. This will cause the isotherms from all subsequent layers to underpenetrate, thereby disturbing the balance of refinement and tempering, and again resulting in an increase in the maximum hardness. Hence, both overgrinding and undergrinding have a negative influence in that they increase HAZ hardness. In simplistic terms, overgrinding promotes "overhardening" and undergrinding promotes "undersoftening," both of which are non-optimum conditions that increase HAZ hardness. Similarly, a decrease in the second layer travel speed increases the second layer thickness, causing the tempering isotherms from the third layer to underpenetrate. Also, an increase in the second layer weld bead overlap increases the second layer thickness, causing the refining isotherms from the third layer to underpenetrate. Each of these effects, overpenetration and underpenetration, results in an increased maximum hardness in the HAZ.

Six-Layer Mechanized GTAW Technique HAZ Structure

The whole of the HAZ produced by the six-layer mechanized GTAW technique has a consistent, highly refined HAZ with a maximum HAZ grain size of 0.015 mm. There is only an extremely low probability of occurrence of local unrefined areas, which is estimated below. The HAZ structures produced are the same as those produced by the half-bead technique, *i.e.*, predominantly martensitic together with a small amount of lower bainite, as shown in Fig. 4.

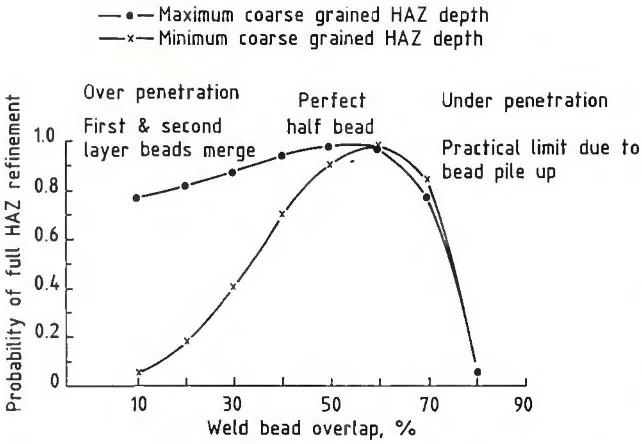

Fig. 8—Effect of weld bead overlap on the probability of obtaining full HAZ refinement using the ASME XI half-bead technique

HAZ Refinement

The six-layer mechanized GTAW technique was designed using the computer model (Ref. 2) and validated (Ref. 5) by depositing carefully controlled, thin layers of weld metal to cause multiple refinement and tempering from successive layers. The layer thicknesses were calculated so as to progressively shift five bands of refining and tempering isotherms up through the first layer HAZ, as indicated in Fig. 5, using two layers as a simple illustration. The principle of refinement and tempering from successive layers is the same for both the half-bead and the six-layer techniques, the major difference being the number of layers involved. Hence, the HAZ refinement sensitivity analysis was approached in the same way. Some additional assumptions were required because of the increased complexity caused by the use of six layers. It was assumed that the variability of the ma-

Table 6—Details of Factorial Experiment Welding Conditions, Calculated Maximum HAZ Hardness and Factorial Analysis of the Effects Produced

Factor		A	B	C	D	E		
Weld No.	Treatment Combination	Travel Sped Layer 1 mm · s^{-1}	Overlap Layer 1 %	Grinding Error mm	Travel Speed Layer 2 mm · s^{-1}	Overlap Layer 2 %	Max Hv	Effect
1	(1)	3.0	40	−0.5	3.2	40	397	—
2	A	3.8	40	−0.5	3.2	40	388	6.4
3	B	3.0	60	−0.5	3.2	40	404	−0.1
4	AB	3.8	60	−0.5	3.2	40	400	4.1
5	C	3.0	40	0.5	3.2	40	402	−8.5
6	AC	3.8	40	0.5	3.2	40	406	11.8
7	BC	3.0	60	0.5	3.2	40	398	−8.5
8	ABC	3.8	60	0.5	3.2	40	409	1.0
9	D	3.0	40	−0.5	4.0	40	393	−8.6
10	AD	3.8	40	−0.5	4.0	40	382	4.6
11	BD	3.0	60	−0.5	4.0	40	398	−0.6
12	ABC	3.8	60	−0.5	4.0	40	399	4.9
13	CD	3.0	40	0.5	4.0	40	358	−6.8
14	ACD	3.8	40	0.5	4.0	40	383	3.3
15	BCD	3.0	60	0.5	4.0	40	364	−0.8
16	ABCD	3.8	60	0.5	4.0	40	390	3.5
17	E	3.0	40	−0.5	3.2	60	419	21.5
18	AE	3.8	40	−0.5	3.2	60	411	1.0
19	BE	3.0	60	−0.5	3.2	60	425	−6.8
20	ABE	3.8	60	−0.5	3.2	60	419	1.0
21	CE	3.0	40	0.5	3.2	60	404	−2.1
22	ACE	3.8	40	0.5	3.2	60	427	0.6
23	BCE	3.0	60	0.5	3.2	60	400	−4.9
24	ABCE	3.8	60	0.5	3.2	60	403	2.1
25	DE	3.0	40	−0.5	4.0	60	419	8.5
26	ADE	3.8	40	−0.5	4.0	60	413	−0.3
27	BDE	3.0	60	−0.5	4.0	60	422	−2.8
28	ABDE	3.8	60	−0.5	4.0	60	422	4.8
29	CDE	3.0	40	0.5	4.0	60	421	6.1
30	ACDE	3.8	40	0.5	4.0	60	421	−0.9
31	BCDE	3.0	60	0.5	4.0	60	368	−2.1
32	ABCDE	3.8	60	0.5	4.0	60	421	5.1

Table 7—Probabilities of Underpenetration, Overpenetration and Refinement for Individual Elements of the Remaining Possible Combinations Taken from Table 7, as a Function of Weld Bead Overlap

Weld Bead Overlap (%)	2UP1	2OP1	2R1	3UP1	3UP2	3OP1	3OP2	3R1	3R2
10	0	0.19	0.81	0	0	0.02	0.10	0.98	0.9
20	0	0.17	0.83	0.01	0	0.01	0.07	0.98	0.93
30	0	0.14	0.86	0.02	0	0	0.05	0.98	0.95
40	0	0.11	0.89	0.05	0	0	0.03	0.95	0.97
50	0	0.07	0.93	0.14	0	0	0.01	0.86	0.99
60	0.01	0.03	0.96	0.43	0.02	0	0	0.47	0.98
70	0.03	0.01	0.96	0.90	0.13	0	0	0.1	0.87
80	0.25	0	0.75	1	0.76	0	0	0	0.24

Note: For the lowest weld bead overlap, say 10%, there is a greater probability that isotherms from Layers 4, 5 or 6 could overpenetrate the reduced layer thicknesses, which would result from the use of a low weld bead overlap. This would imply that Pr(4OP1) and Pr(4R1) might not be equal to zero and the number of possible combinations would therefore increase. However, the probability Pr(4OP1) is 0.001 and Pr(4R1) is 0.079 at 10% weld bead overlap and Pr(4UP1) is 0.920. Since Pr(5OP1), Pr(6OP1), Pr(5R1), Pr(6R1) are less likely, the number of combinations considered that have a nonzero probability of occurrence is nine, as given by Table 7.

Table 8—Combined Probabilities, Generated from Individual Element Probabilities Given in Table 8, for All Possible Successful and Unsuccessful Combinations for Six-Layer Refinement as a Function of Weld Bead Overlap

	Weld Bead Overlap %							
Combination	10	20	30	40	50	60	70	80
1. 2UP1; 3UP1; 4UP1; 5UP1; 6UP1	0	0	0	0	0	0	0.03	0.25
2. 2OP1; 3UP2; 4UP2; 5UP2; 6UP2	0	0	0	0	0	0	0	0
3.[a] 2R1; 3UP1; 4UP1; 5UP1; 6UP1	0	0.01	0.02	0.04	0.14	0.43	0.86	0.75
4. 2UP1; 3OP1; 4UP3; 5UP3; 6UP3	0	0	0	0	0	0	0	0
5. 2OP1; 3OP2; 4UP3; 5UP3; 6UP3	0.02	0.01	0.01	0	0	0	0	0
6. 2R1; 3OP1; 4UP3; 5UP3; 6UP3	0.02	0.01	0	0	C	0	0	0
7.[a] 2UP1; 3R1; 4UP1; 5UP1; 6UP1	0	0	0	0	0	0	0	0
8.[a] 2OP1; 3R2; 4UP2; 5UP2; 6UP2	0.17	0.16	0.13	0.11	0.07	0.03	0.01	0
9. 2R1; 3R1; 4UP1; 5UP1; 6UP1	0.81	0.83	0.86	0.89	0.86	0.47	0.10	0
ΣPr(successful combinations)	0.98	1.00	1.01	1.04	1.07	0.93	0.97	0.75
ΣPr(unsuccessful combinations)	0.04	0.02	0.02	0	0	0	0.03	0.25
ΣPr(successful) + ΣPr (unsuccessful)	1.02	1.02	1.02	1.04	1.07	.93	1.00	1.00

(a) Indicates successful combinations resulting in full six-layer refinement.

Notes: (1) Pr(2UP1; 3UP1; 4UP1; 5UP1; 6UP1) = Pr(2UP1) × Pr(3UP1) × Pr(4UP1) × Pr(5UP1) × Pr(6UP1).

(2) Since the six-layer refinement must either be successful or unsuccessful the total probability, *i.e.*, ΣPr(successful) + ΣPr(unsuccessful) should equal unity. The deviations shown result from rounding errors and the initial assumption that Layers 4–6 always underpenetrate the underlying HAZ thereby reducing the number of possible combinations.

chine-set welding conditions was low and that the resultant changes in weld bead dimensions caused by these systematic errors were negligible with respect to the measured weld bead variability. The main systematic error controlling HAZ refinement was assumed to be the variability in weld bead overlap caused by the difficulty of accurate bead placement in a cavity of complex geometry. This resulted in systematic variations in layer height which could affect the refining capability of all individual layers or combinations of layers. However, this assumption is examined in more detail for extreme value welding parameters.

The method followed to evaluate the probability of successful HAZ refinement for the half-bead technique was also used for the alternative six-layer technique, taking bead placement errors into account as described previously. The probabilities for overpenetration, underpenetration and refinement have been evaluated as a function of weld bead overlap for each layer and possible combination of layers. The following notation has been adopted: 2R1 indicates that the second layer isotherms refine the first layer HAZ. Thus, the sequence 2OP1, 3R2, 4UP2, 5UP2, 6UP2 indicates that the second layer HAZ overpenetrates the first layer HAZ creating a new band of coarse grains; the isotherms from Layer 3 refine this new band of coarse grains; isotherms from Layers 4, 5 and 6 leave the HAZ unchanged in terms of refinement, *i.e.* the isotherms from Layers 4–6 underpenetrate. The probability of 2OP1, 3R2, 4UP2, 5UP2, 6UP2 occurring is calculated from the product of the individual probabilities of each element of the combination. The global probability of success is estimated from ΣPr (successful combinations) which should be equal to 1 − ΣPr (unsuccessful combinations) which can be used as an independent check on the calculations.

Since the second layer can underpenetrate, 2UP1, refine, 2R1, or overpenetrate, 2OP1, the first layer HAZ, there are three possible outcomes. These are combined with three further possible outcomes as each subsequent layer is added, making a total of 243 possible combinations for the six layers as shown in the appendix. Note that if an individual element has a near-zero probability of occurrence, *e.g.*, Layer 6 overpenetrates Layer 1, 6OP1, then all combinations containing this element will also reduce to zero. Those elements which effectively reduce to zero are shown in the appendix. When these are excluded, nine combinations remain. The probabilities of these occurring are shown in Table 7 as a function of weld bead overlap. Combined probabilities for all possible combinations are shown in Table 8.

With one exception, the independent check on the accuracy of the calculations using the total probability shows a slight systematic overestimate, which results from inaccuracies introduced by performing all calculations to two decimal places together with the initial assumption that Layers 4–6 always underpenetrate the underlying HAZ. However, the calculations are sufficiently accurate for comparison purposes and so the values have been normalized against the total probability calculated and plotted in Fig. 9. Since the tolerance to systematic variations in weld bead overlap is high and large variations in each of the welding parameters would be required to produce significant changes in the thickness of individual layers, it follows that the six-layer procedure is highly tolerant to systematic variations in any of the welding parameters. Note that practical limits to the allowable variations in weld bead overlap constrain the permissible values to ≧ 20% to prevent the first and second layer beads from merging and to ≦ 75% to avoid weld bead pile up.

HAZ Hardness

The intent of the six-layer technique is to produce a refined and tempered HAZ which is, in principle, identical to the half-bead technique but with less inherent variability.

The likely control variance during welding in practice has been estimated for each of the major welding parameters. These are ±1 A for welding current, ±1 V for welding voltage, ±0.64 mm · s^{-1} (1.5 in./min) for wire feed speed, ± 0.34 mm · s^{-1} (0.8 in./min) for travel speed and ± 0.5 mm (0.02 in.) for control of bead placement. These figures represent engineering estimates of maxima and minima and relate to the 95% confidence limits, which represent $\pm 2\sigma$.

Additional lengthy computation would be needed to estimate the combined effects of systematic errors in the machine settings and control variance deterioration on HAZ hardness for each individual welding parameter for each of the six layers. However, the six-layer technique has a better chance of successfully refining and tempering the underlying HAZ than the half-bead technique, which essentially relies on three layers to refine and temper, given that the first layer HAZ's for the SMAW and GTAW processes are not substantially different.

Systematic errors in the machine settings are unlikely to be substantial for calibrated equipment and any errors would be present for each of the six layers. The sensitivity of the six-layer procedure to systematic weld parameter variation was estimated using the computer model to consider each welding parameter in isolation, ignoring any possible interactive effects and additional contributions from the control variance. In addition, the weld bead variabilities were artificially set to zero to eliminate system noise, which would otherwise complicate the interpretation of the measured responses. Maximum HAZ hardnesses across the HAZ were calculated for each of three characteristic positions: at the cusp between two beads, at the position of maximum first-layer penetration and at the position midway between the first two positions.

The welding parameter systematic deviations used and the calculated HAZ hardness maxima that resulted at each of the three characteristic HAZ positions are given in Table 9. Note that these values represent deviations from the welding conditions given in Table 4. In addition, the same systematic deviation in each of the welding parameters was assumed to be present in each of the six layers. The results show that the systematic deviations that produce minimum HAZ hardnesses within the range 295–345 Hv as defined by the calculated hardness envelope given in Fig. 3 are of the order: −70 to +150 A for the welding current; ±1.5 mm · s^{-1} (3.5 in./min) for the welding travel speed; ±12.5 mm · s^{-1} (30 in./min) for the wire feed speed, −40 to +20% for weld bead overlap and −50° to +200°C (−90° to +360°F) for preheat and interpass temperatures from each of the respective mean values. The tolerance to variation in welding voltage will be of the same order as the tolerance to current variation, *i.e.*, −4.3 to +9 V from the mean value. These estimates assume that only one systematic error is present for each weld and takes no account of possible interactive effects. In addition, the welding conditions are extreme values outside the empirical database and must be viewed with caution. However, the general indication is that the six-layer technique is extremely tolerant to systematic errors.

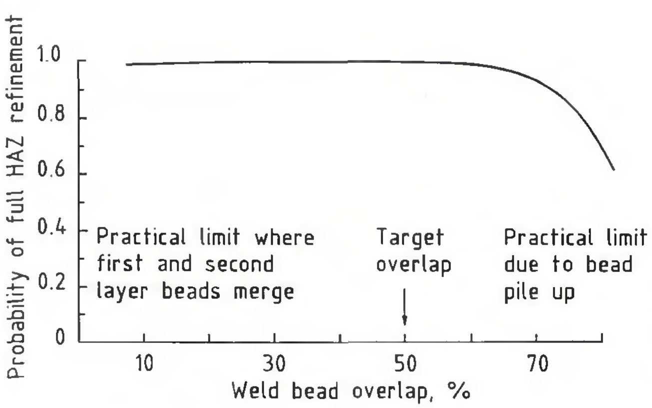

Fig. 9—Effect of weld bead overlap on the probability of obtaining full HAZ refinement using the alternative six-layer GTAW technique

Control variance deterioration, *i.e.*, the increasing variability of any welding parameter once set at a required value, will contribute to the overall variability of the weld bead dimensions, thereby reducing the tolerance of the process. The contribution is expected to be low for modern welding equipment. The observed scatter in the measured HAZ hardness traverse values includes contributions from weld bead variability and weld parameter variability, and is of the same order as the calculated scatter, which took into account the effects of weld bead variability alone. This indicates that the welding parameter control variance contribution is minor. This is reinforced by the following simplified arguments.

The bead width variability has a standard deviation of 0.63 and mean bead

Table 9—Maximum HAZ Hardness Produced by Systematic Deviations from the Six-Layer Alternative Procedure Welding Condition (Ref. 5)

Welding Parameter	Value	Systematic Deviation	HAZ Position: Cusp	HAZ Position: Intermediate Position	HAZ Position: Maximum Penetration
Current A	130	−70	341	342	332
	150	−50	343	343	327
	170	−30	343	345	340
	180	−20	334	339	341
	200[a]	0	316	331	335
	270	70	317	317	310
	350	150	304	319	334
Travel speed mm · s^{-1}	0.96	−2.0	276	278	280
	1.46	−1.5	297	297	302
	1.96	−1.0	321	322	328
	2.96[a]	0	316	331	335
	3.96	1.0	343	334	331
	4.46	1.5	333	332	345
	4.96	2.0	333	349	347
Weld bead overlap %	10	−40	300	300	300
	20	−30	303	299	302
	50[a]	0	316	331	335
	70	20	329	319	340
	75	25	346	336	339
	80	30	373	363	360
Wire feed speed mm · s^{-1}	6.2	−15	352	373	363
	8.7	−12.5	313	318	316
	11.2	−10	308	313	321
	21.2[a]	0	316	331	335
	31.2	10	333	325	316
	33.7	12.5	341	332	323
	36.2	15	348	339	329
	41.2	20	353	347	332
Preheat or interpass temperature °C	50	−100	325	344	350
	100	−50	320	338	343
	150[a]	0	316	331	335
	250	+100	307	317	321
	350	+200	296	300	304

Notes: (1) All welding parameter combinations resulted in 100% refinement.
(2) Systematic deviations for each welding parameter apply to all six layers.
(a) Indicates the mean value from Table 4.

width and gross heat input have a correlation coefficient of 0.95—Equation 5. Bead height is inversely correlated with bead width, hence the bead width-welding parameter relationship given by Equation 5 together with the correlated bead height value, Equation 7, can be used to estimate the sensitivity to control variance deterioration for each welding parameter in isolation. The percentage variations required to produce values of bead width, bead height or the equivalent change in layer height two standard deviations from the mean are 23% for current, 23% for voltage, 23% for travel speed, 25% for wire feed speed and 13% for weld bead overlap. In comparison, typical control variance values are 0.5% for current, 10% for voltage, 11% for travel speed, 2.5% for wire feed speed and 11% for weld bead overlap. Note that all percentage values refer to second layer conditions, which represent an average condition of welding parameters used—Table 4.

Discussion

The ASME XI half-bead technique and the mechanized six-layer alternative technique both use a layer-by-layer refinement and tempering technique to progressively heat treat the HAZ produced by the first layer weld deposit.

Both techniques produce identical HAZ transformation products, which are fine-grained martensitic structures together with a small proportion of lower bainite with a typical HAZ grain size of 0.015 mm. However, there is a 3-8% probability that some isolated coarse-grained regions with a grain size of 0.1 mm may be produced due to the greater variability associated with the manual ASME XI half-bead technique. The probability of occurrence of these coarse-grained regions is sensitive to uncontrolled variations in ground layer height. This sensitivity can be expressed in terms of a tolerance limit, which represents a 50% chance of obtaining islands of coarse unrefined HAZ structures. These tolerances are −0.6 mm and +1.1 mm for target ground layer height. The procedure is not sensitive to variations in welding current, welding voltage, welding travel speed or weld bead overlap in the range 35-75%, providing the same systematic errors are present in both layers.

The HAZ refinement produced by the mechanized six-layer technique is also insensitive to variations in welding parameters. Weld bead overlap is the most critical parameter for repair situations in a cavity of complex geometry. Even so, the procedure can tolerate variations in weld bead overlap in the range 20-75%, the allowable variations being set by practical considerations.

Both techniques involve significant tempering during welding, which reduces the initial peak HAZ hardnesses from 450 Hv to final tempered hardnesses with calculated means of 345 and 320 Hv for the half-bead and six-layer techniques, respectively. The main difference between the two techniques lies in the sensitivity to welding parameter variations. The ASME XI half-bead technique may contain patches of coarse, unrefined HAZ structures and the same sensitivity is also reflected in the tempering response in that there may be isolated patches of HAZ that are not fully tempered. These patches will have maximum dimensions of order 0.5 bead width × 0.5 refining depth in cross-section and could extend for the run-out length of a single weld bead. Typically, these dimensions would be 4 × 2 mm (0.2 × 0.1 in.) in cross-section with a maximum possible length of 400 mm (16 in.). The occurrence of these hard patches is encouraged by overgrinding, slow second layer travel speed and high second layer weld bead overlap, which are operator dependent. Typical hardness scatter is calculated to be ± 50 Hv for the half-bead technique if hard spots are present. In the absence of hard spots, it is calculated that the mean final tempered hardness will be reduced to ~ 330 Hv with a scatter of ± 30 Hv, which is comparable with the six-layer technique. The six-layer technique is likely to be highly tolerant to systematic weld parameter variations and to changes in control variance. This implies that there will be a range of six-layer techniques that would perform as satisfactorily as the particular variant examined in this report. In effect, this offers greater flexibility for practical applications in that general nonspecific guidelines could be formulated, which would allow an individual fabricator the freedom to design any particular six-layer weld procedure thought to offer some practical advantage. This would have the additional advantage that the onus of responsibility for success of the procedure would rest with the fabricator and not with the ASME XI code authorities (Ref. 11).

Conclusions

1) The heat-affected zone grain size produced by both techniques is typically 0.015 mm with predominantly martensitic structure. Computer model calculations show that the refinement produced by both techniques is not sensitive to systematic or random variations in welding parameters. However, the ASME XI half-bead technique has a 3-8% chance of producing isolated, unrefined islands with a grain size of 0.1 mm. The probability is increased to 50% by manual grinding errors to the first layer height of −0.6 and +1.1 mm (−0.2 and +0.04 in.).

2) The ASME XI half-bead technique mean hardness produced is sensitive to the thickness of individual layers of weld beads. In particular, isolated hard spots of ~ 400 Hv are promoted by overgrinding of the first layer, slow second layer travel speed and high second layer weld bead overlap, which are operator-dependent parameters.

3) The six-layer technique mean hardness produced is extremely tolerant to systematic errors in any of the welding conditions and is not sensitive to the control variance typical of modern welding equipment. This tolerance implies that a range of welding conditions could be specified for each of the six layers so as to maintain the refinement and tempering action during the deposition of successive layers.

Appendix

Possible Layer-By-Layer Combinations for Six- Layer Refinement

Layer 2		Layer 3		Layer 4		Layer 5		Layer 6
2UP1		3UP1		4UP1		5UP1		6UP1
2OP1	×	3OP1	×	4OP1	×	5OP1	×	6OP1
2R1		3R1		4R1		5R1		6R1

Note: 1) There are 3 possible combinations for each layer, making a total of 243. 2) The nomenclature for second layer isotherms overpenetrating the HAZ produced by the first layer; third layer isotherms refining the HAZ; fourth layer and all subsequent isotherms underpenetrating the HAZ is

2OP1; 3R2; 4UP2; 5UP2; 6UP2.

This sequence is required because the original first layer HAZ is replaced by a second layer HAZ whose dimensions reflect the welding conditions used for the second layer. Consequently, the third layer provides refinement for the appropriate second layer HAZ.

3) After deposition of the first three layers using the welding conditions given in Table 4, with a weld bead overlap of 50%, the isotherms from Layers 4, 5 and 6 will almost certainly underpenetrate the underlying HAZ. Consequently, there is an extremely low probability of refinement or overpenetration for the isotherms of Layers 4, 5 and 6, *i.e.*

$$Pr(4OP1) = Pr(5OP1) = Pr(6OP1) = 0$$
and $$Pr(4R1) = Pr(5R1) = Pr(6R1) = 0$$
and conversely
$$Pr(4UP1) = Pr(5UP1) = Pr(6UP1) = 1.$$

Since the probability of a given combination occurring is given by the product of the probabilities of each of the individual elements, all combinations which contain 4OP1, 5OP1, 6OP1, 4R1, 5R1 and 6R1 will have a near-zero probability of occurrence and can be eliminated from the total possible combinations. 4OP2, 5OP2, etc., also have a near zero probability of occurrence since the sequence indicates that the second layer HAZ isotherms over-penetrated the first layer HAZ so that the second layer HAZ must occupy a similar spatial position to the first layer HAZ which it replaced. Hence, the isotherms from Layer 4 almost certainly underpenetrate the second layer HAZ. Hence, the remaining possible combinations are:

1. 2UP1; 3UP1; 4UP1; 5UP1; 6UP1
2. 2OP1; 3UP2; 4UP2; 5UP2; 6UP1
3. 2R1; 3UP1; 4UP1; 5UP1; 6UP1
4. 2UP1; 3OP1; 4UP3; 5UP3; 6UP3
5. 2OP1; 3OP2; 4UP3; 5UP3; 6UP3
6. 2R1; 3OP1; 4UP3; 5UP3; 6UP3
7. 2UP1; 3R1; 4UP1; 5UP1; 6UP1
8. 2OP1; 3R2; 4UP2; 5UP2; 6UP2
9. 2R1; 3R1; 4UP1; 5UP1; 6UP1

References

1. Alberry, P. J., and Lambert, J. A. 1982. The welding metallurgy of SA508 Class 2 heat-affected zones. *Int. Conf. on Welding Technology for Energy Applications, Session 5,* Oak Ridge National Laboratories, Oak Ridge, Tenn.

2. Alberry, P. J. 1985. *A Computer Model for the Calculation of Heat-Affected Zone Hardness in Multipass Repair Welds in SA508 Class 2.* CEGB Report TPRD/M/1474/R85.

3. Alberry, P. J., and Jones, W. K. C. 1982. Computer model for prediction of heat-affected zone microstructures in multipass weldments. *Metals Tech.* 9(10):419–426.

4. Alberry, P. J., Brunnstrom, R. R. L., and Jones, K. E. 1983. Computer model for predicting heat-affected zone structures in mechanized tungsten inert gas weld deposits. *Metals Tech.* 10(1):28–38.

5. Babcock & Wilcox. 1984. *Repair Welding of Heavy Section Steel Components in Light Water Reactors.* EPRI NP-3614 Final Report, Project 1236-1.

6. Cramer, H. 1946. *Mathematical Methods in Statistics.* Publ. Princeton Univ. Press.

7. Davies, O. L. 1958. *Statistical Methods in Research and Production.* Publ. Oliver and Boyd, London.

8. Pelli, R., and Rintamaa, R. Properties of heat-affected zones in repair welds of pressure vessel steels. DVS Berichte No. 75, *Proc. 4th Int. Conf. on Welding in Nuclear Eng.,* Aachen, Germany, pp.49–52.

9. Higuchi, M., Sakamoto, H., and Tanioka, S. 1980. A study on weld repair through half bead method. *I. H. T. Eng. Rev.* 13(2):14–19.

10. Davies, O. L. 1960. *The Design of Industrial Experiments.* Publ. Oliver and Boyd, London.

11. Alberry, P. J., and Feldstein, J. G. 1985. Alternatives to half-bead repair technique. *International Conference on Maintenance Welding in Nuclear Power Plants, III,* Knoxville, Tenn.

Acknowledgments

Funds for this work were supplied by EPRI under contract RP 1757. The contributions of Mr. R. R. L. Brunnstrom (MEL), Mr. J. G. Feldstein (Babcock and Wilcox) and Dr. R. E. Nickell (EPRI) are gratefully acknowledged.

The work was carried out at the Marchwood Engineering Laboratories of the Technology Planning and Research Division and the paper is published with permission of the Central Electricity Generating Board.